A Microwave Decoupled Electrode for the Electroencephalogram

L. E. LARSEN, R. A. MOORE, SENIOR MEMBER, IEEE, AND J. ACEVEDO

Abstract—**The recording of the electroencephalogram (EEG) in an amplitude-modulated microwave field presents two related but distinct problems when conventional electrodes are employed. The electrode and its associated conductors extract power from the incident radiation, resulting in increased local power deposition which confounds dosimetric arguments and imposes local thermalization; the electrode tissue interface is a nonlinear system that demodulates amplitude-modulated signals with the results that the demodulate is additively mixed with the EEG.**

The problems were studied in a series of bench tests with conventional and thin-film microwave integrated circuit (MIC) electrodes. The latter are decoupled from the magnetic component of the field by virtue of radically reduced dimensions of the thin-loop component of its geometry, and suppression of dipole (i.e., electric field interaction) currents by use of integrated Nichrome series resistance. The result is that the demodulation artifact is undetectable in the ensemble averaged-power spectrum from the *in vitro* electrode up to an *S*-band incident-power density of 100 mW/cm². Thermalization was studied in a dielectric brain phantom with high-resistance monofilament leads to the MIC with a result that 0.6°C heating is attributable to the electrode with prolonged exposure to a 50-mW/cm² field.

INTRODUCTION

A study of microwave effects on the central nervous system (CNS) may measure any one of a number of electrophysiological responses to irradiation. If the objective is to study the time course of microwave effects in an unanesthetized animal, measurement of the electroencephalogram[1] would figure prominently in the design.

Measurement of the electroencephalogram in a microwave field presents at least two problems. First, the conventional chronic EEG electrode employs either metallic skull screws or small (e.g., 5-mil) wires in nonmetallic skull screws as the electrode(s). The presence of conventional conductors immediately raises the issue of increased power absorption and its subsequent effects, notably brain heating. Indeed it is possible, after irradiation with power densities as low as 20 mW/cm², to detect lesions in the brain scan which are localized under metallic skull screws (Larsen and Johnson, in preparation).

Secondly, there is considerable interest in the use of amplitude-modulated RF with modulation frequency within the EEG bandwidth. The question is whether or not amplitude-modulated RF can induce alterations in the EEG which are related to the modulation frequency, which in turn presents still another measurement problem, since the electrode–tissue interface is a nonlinear system. That is, the RF may be demodulated at the electrode–tissue interface, with the result that the demodulate is mixed with the EEG and is interpreted as changes in the EEG. There are several indirect and inconclusive methods for dealing with this problem; however, a systematic method for evaluation of demodulation artifact has not previously appeared. A definitive solution to the problem of demodulation artifact must include such a method and a suitable demonstration of the performance limits of candidate electrodes in terms of incident power and detectable demodulation.

By analogy with a previously developed microwave integrated-circuit (MIC) electrode for brain-temperature measurement [1], we proceeded on the premise that effects due to RF incident on the electrode–tissue interface are several orders of magnitude below that attributable to the additional RF due to antenna-like properties of conductors subsequent to the actual transducer. Thus demodulation artifact may be reduced through decoupling, thereby limiting such additional RF at the electrode–tissue interface. This short paper reports our experience with *in vitro* methods for evaluation of thermal performance and demodulation artifact for conventional and microwave integrated-circuit EEG electrodes.

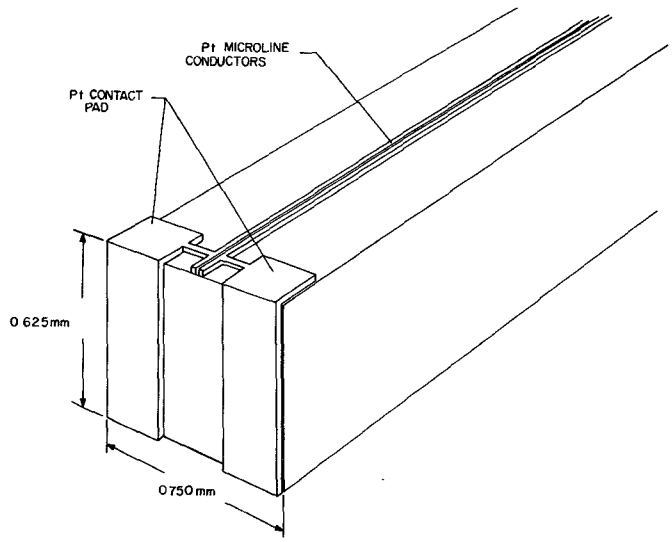

Fig. 1. Conductor layout for the transducer end of the EEG electrode stub. The dimensions are approximate, and the drawing is not to scale.

ELECTRODE CONFIGURATIONS

The first electrodes to be tested were a pair of conventional 6-32 by 1/4-in stainless-steel skull screws cf. [3]. The next candidate consisted of a 5-mil tungsten wire which was insulated everywhere except for a transverse cut at the tip. These electrodes were held in a pair separated only by the thickness of the insulation. The MIC electrode consisted of thin-film (evaporated Cr followed by Pt) conductors 5-μm wide with a 5-μm separation on a stub (3/8 in long) of sapphire substrate.[2] The part that contacted the dura consisted of two pads 10 mils square separated by 10 mils (cf. Fig. 1).[3] The remainder of the microcircuitry was passivated. The stub was connected to an upper substrate square, which contained current-limiting resistors of various configurations, in a number of ways. The first version attached the stub to a Teflon carrier on the upper substrate square. Contact from the stub to 50-kΩ flip-chip resistors on the upper substrate was made by 1-mil gold wire. The second version attached the stub to the flip-chip resistors by face-to-face contact with gold miniballs and thermal-compression bonding. Versions three and four used the same method of attachment but added 50-kΩ Nichrome thin-film resistors on the upper substrate with and without, respectively, the flip-chip resistors. The upper substrate also carried larger contact pads to which high-resistance line was attached. The line was either directly connected to the pads (cf. [1] for details), or it was terminated in 1-mil gold wire that was then bonded by thermal compression to the pads. Conductors subsequent to the upper substrate were of two varieties. The first consisted of conductive monofilament with 15-kΩ/ft resistance (cf. [1] for details). The second material was a sandwich of two strips of planar ultrahigh-resistance line[4] on either side of Teflon-backed double-sided adhesive.[5] We identify this sandwich as bifilament; its resistance was approximately 100 kΩ/ft.[6] The MIC was then plotted

Manuscript received January 28, 1974; revised May 30, 1974. Some of the contents of this paper were presented at the IEEE PGMTT International Symposium, Boulder, Colo., June 1973.

L. E. Larsen was with the Walter Reed Army Institute of Research, Washington, D. C. 20512. He is now with the Neurophysiology Department, the Methodist Hospital and the Baylor College of Medicine, Houston, Tex. 77025.

R. A. Moore and J. Acevedo are with the Westinghouse Electric Corporation, Baltimore, Md.

[1] More correctly, the electrocorticogram, if the electrode is located on the cortex rather than the scalp.

[2] Later models employed 2-μm conductors separated by 2 μm.

[3] EEG may be recorded from metallic microelectrodes (1-MΩ source impedance) as close as 30 μm [2].

[4] This line was carbon-loaded tetrafluoroethylene.

[5] We are indebted to Ronald Bowman (NBS, Boulder, Colo.), who kindly provided us with samples of the bifilament.

[6] Only a few inches of the line need be interposed between the upper substrate square and small conventional conductors.

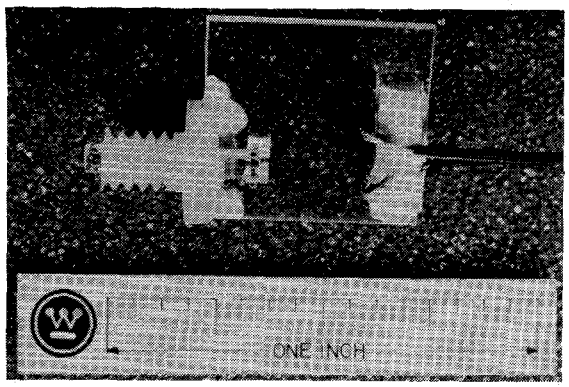

Fig. 2. The completed stub and upper substrate with flip-chip and thin-film Nichrome integrated resistors. The upper substrate contains four pairs of Nichrome lines, only one of which is used. The final product would separate a single pair by cleavage.

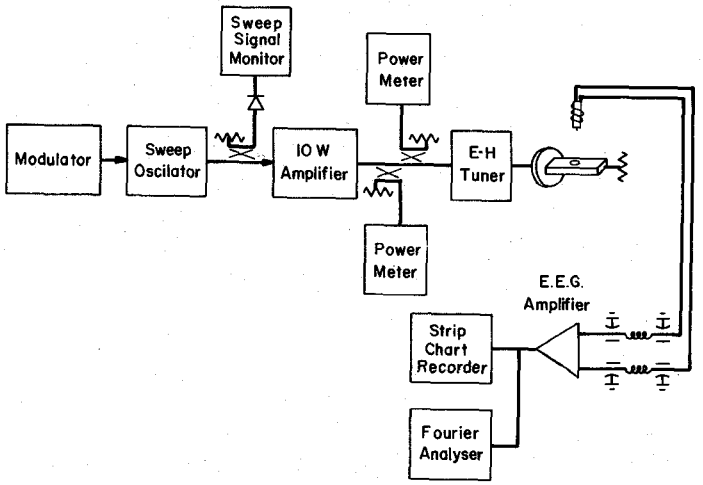

Fig. 3. Functional block diagram of the demodulation testing method.

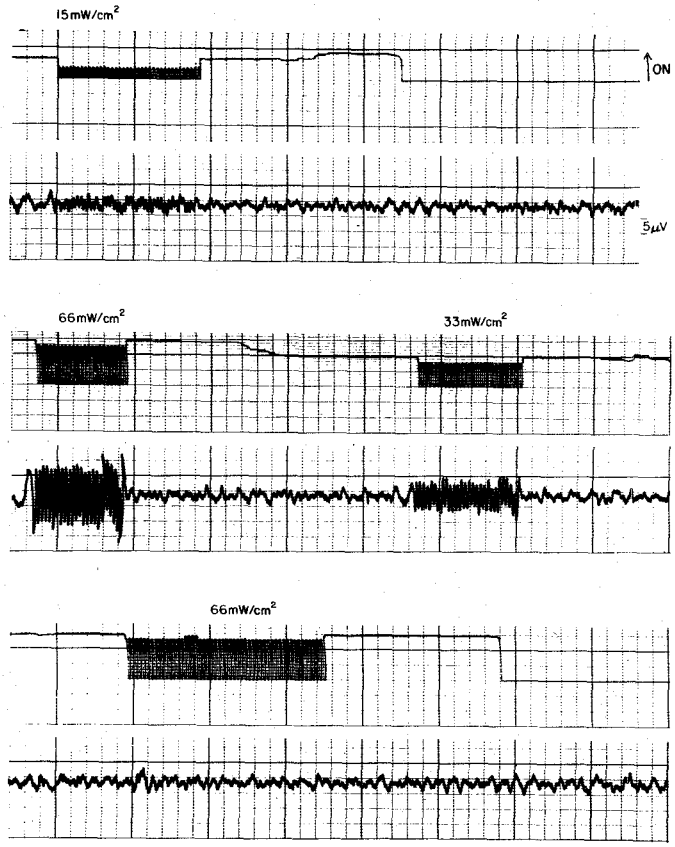

Fig. 4. Strip-chart records which show the comparative performance of 5-mil tungsten wire (top two pairs of tracings) and the MIC electrode (bottom pair of tracings). In each pair, the upper one is the output of a crystal detector (up is on), and the lower one is the output of the differential amplifier. The numbers refer to the power density in milliwatts/centimeters squared.

in a 6-32 by 1/4-in nylon screw for mechanical attachment to the skull as in Fig. 2.

METHODS OF EVALUATION

The candidate electrodes were tested in two environments: 1) waveguide bench tests for demodulation artifact; and 2) free-field exposure for thermal performance. The demodulation testing (cf. Fig. 3 for a block diagram) took place in a saline-filled glass test chamber that was placed in the center of a short section of waveguide. The waveguide section containing the test chamber was terminated in a matched load and preceded by an E-H tuner with a coax to waveguide adapter. This arrangement was powered by a 10-W linear amplifier and amplitude-modulated signal source with suitable couplers and power meters for transmitted and reflected power. Reflections from the load were balanced to zero, by means of the E-H tuner, before each run. The electrode was connected by miniature coax to LC pi section low-pass filters (f_c = 3 GHz, −80 dB at 10 GHz) and thence into a bandpass filter (1/2–30 Hz), differential amplifier, and a strip-chart recorder.

One hundred percent amplitude modulation was employed at several frequencies from 3–12 Hz on a 2450-MHz carrier. Power density varied from 5 mW/cm²–250 mW/cm², depending on the electrode. All electrodes were carried in a micromanipulator to control geometry and penetration in the test chambers. They were circularly oriented for maximum coupling.

When demodulation artifact was not easily evident on visual examination of the strip-chart record, the method of power spectral density (PSD) analysis was employed to detect changes in the output of the differential amplifier at the frequency of modulation. This method employed a Hewlett-Packard 5451A Fourier analyzer with hard-wire telemetry from the amplifier. The signals were low-pass filtered by Khron Hite filters with f_c = 32 Hz.[7] Analog-to-digital conversion was set in the frequency-resolution mode with Δf = 1 Hz and N = 64. Thus the Nyquist frequency was 32 Hz. One hundred samples of the PSD were ensemble averaged, then plotted.

Thermal testing took place in a 3-ft³ anechoic chamber. The target consisted of a 3-cm (radius) hemisphere filled with dielectric material approximating brain at 3 GHz [4]. The target with and without the electrode was heated in a field of 50-mW/cm² power density by means of an open-ended waveguide with flange, E-H tuner, and Burdick 200-W diathermy source at 2460 Hz. The pattern of power absorption by the target with and without the electrode was compared with infrared thermography (cf. [1] for further discussion). The thermograph was calibrated by means of a laboratory standard differential (Δt) blackbody radiator in order to verify the accuracy of the quantified displays.

RESULTS

The MIC electrode effectively suppressed demodulation artifact, as shown in Fig. 4. The stainless-steel skull screws were found to demodulate visibly[8] in a 20-mW/cm² field. The 5-mil wire demodulated visibly in a 15-mW/cm² field but not in a 5-mW/cm² field. However, PSD analysis of the amplifier output showed changes in the noise spectrum at demodulation frequencies (cf. Fig. 5).

The 5-μm MIC did not demodulate visibly until a power density of approximately 200 mW/cm². Power spectral analysis detected demodulation at 90–110 mW/cm², depending on the particular electrode sample, as shown in Fig. 6.

[7] These filters were operated in cascade fashion with a roll-off of 96 dB/8 ave.

[8] Visible demodulation means that the prior signal (RF on without amplitude modulation) is totally obscured by modulation envelope.

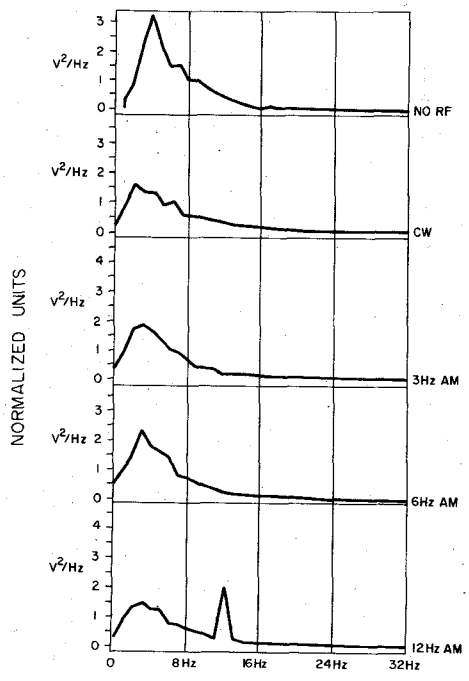

Fig. 5. Power spectral density (PSD) analysis of the amplifier output for the 5-mil wire electrode at 5-mW/cm² power density. Each curve is the ensemble average of 100 trials, each 1-s long. The upper curve is the PSD with no RF, the second one with continuous wave (CW) 2450 MHz, and the next three with 3-, 6-, and 12-Hz amplitude modulation.

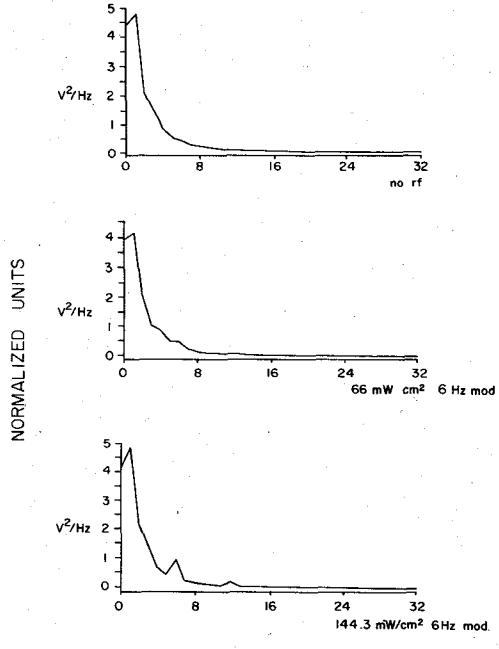

Fig. 6. Power spectral density analysis of the 5-μm MIC electrode under three conditions. Note the presence of the second harmonic of the modulation frequency in the 144-mW/cm² case.

The results of thermographic examination of the MIC electrodes varied with the type of construction. In all versions, the conductive monofilament (15 kΩ/ft) demonstrated its usual 10°C mode of heating at a distance of approximately 2 cm from the upper substrate after 30–60 s of heating in a 50-mW/cm² field. Other sources of thermalizing interaction with the field included the use of 1-mil Au point-to-point wiring in version one and the use of flip-chip resistors in versions two and three.

That is, version one provided thermal isolation between the needle and the current-limiting resistors but introduced an independent heating of 1.5–2.0°C at the transducer in a 50-mW/cm² field after thermal equilibrium. Version one heated about 0.6°C even with the monofilament removed. Unlike the former design, versions two and

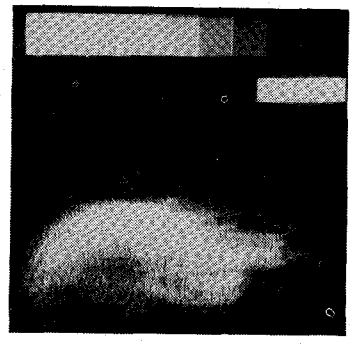

Fig. 7. Thermograph of version four MIC electrode in the phantom after prolonged heating in a 50-mW/cm² field. The monofilament is removed. The display is quantized in 0.3°C steps with isometric enhancement.

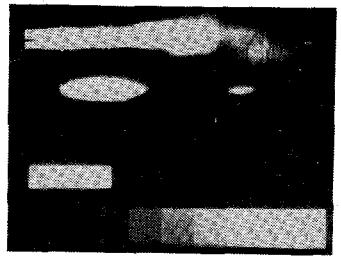

Fig. 8. Thermograph of version four MIC with 15-kΩ/ft monofilament and BeO_2 heat sink after several minutes of exposure. The display is quantized in 0.3°C steps without isometric enhancement. The spheroids at the left center are marker pieces of monofilament. The upper one corresponds to the heat sink, and the lower one corresponds to the electrode stub.

three performed well with the monofilament removed but heated to about 1°C underexposure with the monofilament attached. Version three gave the best performance in the absence of the monofilament, being essentially undetectable under those circumstances as seen in Fig. 7, but once again heated to about 1°C after prolonged exposure with the monofilament attached.

When a 5-cm section of ultrahigh-resistance bifilament ($\simeq$100 kΩ/ft) was interposed between the upper substrate square and the 15-kΩ/ft line, the problems of proximal line heating and thermal diffusion were solved. However, the needle itself was now heated to about 0.5–1.0°C against a picture of cold proximal line and upper substrate. A return to the 15-kΩ/ft line with a BeO_2 heat sink produced about 0.6°C heating in a 50-mW/cm² field after long enough periods of exposure to reach the thermal equilibrium (cf. Fig. 8). Heat produced during the first 30–60 s of exposure was limited to about 0.1°C. The application of forced air to the heat sink prevented any temperature rise in the electrode, but it conducted heat out of the target in the vicinity of the needle.

DISCUSSION

The MIC design was based on earlier theoretical considerations of decoupling discussed in Larsen *et al.* [1]. Briefly, the electrode's geometry provides the means of power extraction from the field as an antenna with thin loop and short dipole components. The experimental approach to these properties employed thin-film photolithographic conductors to reduce loop area and integrated resistors for limiting dipole currents. This strategy did effectively suppress demodulation artifact such that the electrode could operate in power densities up to 100 mW/cm² with no detectable (in the power spectrum) demodulation.

It may be argued that this method of demodulation-artifact evaluation is too demanding in the sense that in actual application the amount of artifact is comparable to the noise level and will be well below the EEG signals. We believe this philosophy is misleading and counterproductive on at least three grounds.

1) The quantitative level of the artifact may be easily 6–12 dB over the noise floor, depending on the specific electrode, the relative geometry of the target and the field, and the power level employed. Under the right set of circumstances (good electrode coupling, adequate incident power, and low-voltage endogenous EEG), the artifact could visibly penetrate into the record for various lengths of time and be interpreted as a microwave-induced effect.

2) Most experimental approaches to the neurophysiological problem of measuring alteration of the EEG would employ time-series analysis to detect changes in EEG. Such methods as auto-power and cross-power spectral density analysis are extremely sensitive extractors of signal from noise. It is just this condition that would capitalize on low-level systematic signals that arise from demodulation artifact.

3) The only way to insure a high level of confidence in the results of such an experiment is to demonstrate, in conditions that maximize its detection, the absence of demodulation artifact.

The thermal performance would appear to be limited to, at best, a 1/2°C heating in a 50-mW/cm² field for exposure periods longer than 30–60 s. This is somewhat disappointing, especially, since the ultrahigh-resistance line (bifilament) solved the thermal-diffusion problem. We cannot offer a good explanation of why the bifilament caused the microline to heat.[9] The BeO_2 heat sink would offer some promise for short-exposure durations. If forced air were employed, the length of exposure could be increased to thermal equilibrium, but then the question of removing heat from the brain, skull, and scalp must be considered.

Possible future approaches would include microline that has higher resistance or is longer or both, along with reduced surface area for the platinum transducer pads. Heat sinking and more thermal mass probably offer little promise, since they only seem to delay the eventual development of problems.

This discussion may show a deficiency of the model used for thermal testing; that is, the heat capacity of the head phantom is limited, due to the absence of cerebral circulation. Further, the thermal gradients are unrealistic in the model as compared to a real head. For example, in the model the phantom begins at uniform temperature, whereas in the head, deep brain is warmer than surface brain, and both are warmer than the skull and scalp. In other words, the 1/2°C heating at the electrode needle may represent an extreme that could be reduced if the model were improved to include more realistic thermal gradients and thermodynamics. Of course, these arguments could be applied to the nondecoupled electrode as well. The issue is merely that, in its present state, the thermodynamics of the phantom are more rigorous than those of the animal. In other words, the phantom provides for a dosimetric mapping of fields within a target; it does not model thermoregulation. Nevertheless, the present electrode does modify power absorption, although the perturbation it introduces is much reduced in comparison to that associated with conventional conductors (cf. [1], [5]).

CONCLUSION

The 5-μm MIC electrode is free from demodulation artifact (as detectable in the PSD) at power densities up to 100 mW/cm². Conventional electrodes of small surface area (5-mil diameter W wire) demodulated at 5 mW/cm². The MIC electrode and monofilament with BeO_2 heat sink heated less than 0.1°C for the first 30–60 s of exposure in a 50-mW/cm² field. After several minutes of exposure, when thermal equilibrium is established, the electrode heats about 0.6°C. Ultrahigh-resistance line (bifilament) reduced lead heating and thermal diffusion to negligible proportions but enhanced needle heating.

ACKNOWLEDGMENT

The authors wish to thank P. E. Shoaf for his technical assistance.

REFERENCES

[1] L. E. Larsen, R. A. Moore, and J. Acevedo, "A microwave decoupled brain-temperature transducer," *IEEE Trans. Microwave Theory Tech.*, vol. MTT-22, pp. 438–444, Apr. 1974.
[2] R. Elul, "Dipoles of spontaneous activity in the cerebral cortex," *Exp. Neurol.*, vol. 6, pp. 285–299, 1962.
[3] L. E. Larsen, "Brain temperature and EEG data acquisition from animals during microwave exposure," in *Dig. Papers, Joint U. S. Army/Georgia Inst. of Tech. Microwave Dosimetry Workshop*, 1972, pp. 4–9.
[4] A. W. Guy, "Analyses of electromagnetic fields induced in biological tissues by thermographic studies on equivalent phantom models," *IEEE Trans. Microwave Theory Tech. (Special Issue on Biological Effects of Microwaves)*, vol. MTT-19, pp. 205–214, Feb. 1971.
[5] J. F. Lehmann, A. W. Guy, B. J. Delateur, J. P. Stonebridge, and C. G. Warren, "Heating patterns produced by short wave diathermy using helical coil applicators," *Arch. Phys. Med. Rehabil.*, vol. 49, pp. 193–198, 1968.

[9] Currents in the microline are not transmitted without loss to the brain interface due to an impedance discontinuity at the pad-microline junction. Fringe effects from the edge thickness of the pads may be troublesome, but the 40–60-mil spot size of spatial resolution for the thermograph can detect all but the smallest of thermal point sources from the 20 mils of combined pad dimension.

Error in Impedance Measurement When the Signal is Introduced Across the Slotted-Line Probe

JESÚS BARBERO

***Abstract*—For some special applications impedance measurements have to be made where the test level reaching the unknown must be kept very low. In such cases, using slotted-line techniques, the detector and generator are reversed in the test setup, and the test signal is introduced across the probe of the slotted line which is terminated on one side with the load, and on the other with the detector. This short paper briefly describes this familiar method and then discusses the error calculation in the measurement of VSWR and phase when the detector is not perfectly matched.**

I. INTRODUCTION

The classical impedance measurement with the slotted line needs a signal level strong enough to excite a meter after detection. Nevertheless, when the signal level reaching the unknown must be kept very low (e.g., as is the case of active element measurements) it happens that the available energy is insufficient to excite the meter, even a standing wave ratio meter. In such cases, it is possible to change around the generator and detector [1]–[3], introducing the signal across the slotted-line probe. With this arrangement, an increase in sensitivity results because detection is carried out using the signal level right in the line and not across the coupling of the probe where the signal is weaker. Another advantage of this arrangement is that it is possible to work with a well-decoupled probe, because we are only limited by the power that we can get from the generator to have the desired level in the line. In this way the influence of the probe on the measurement is avoided.

If the detector is not perfectly matched, the incident signal on it will be partially reflected and will add vectorially with the excited wave in the probe plane. So the incident wave in the load depends on detector reflection coefficient and on probe position.

In this short paper, the possible errors in the VSWR and in the phase measurement as a function of detector mismatch are calculated so that it is possible to determine the accuracy with which the detector must be matched depending on the desired precision of the measurement.

II. FORMULATION OF THE PROBLEM

Let us consider the two parallel lines as in Fig. 1. In this figure x and y are the distances to probe plane AA', variables with probe displacement, but always keeping $x + y = l$ (l being the electric distance between load and detector).

As it has already been stated, we can work with a well-decoupled probe and so the electromagnetic state of the line will not influence the generator nor, consequently, the excitation voltage. Thus, in each line (X or Y), the incident wave, i.e., the propagating wave in the positive sense (OX or OY), will be the vectorial addition of the excited wave by the probe and the reflected wave arriving from the other line (Y or X). So we can only consider one incident wave and one reflected wave and they are related by the reflection coefficients Γ_x and Γ_D.

Thus, with the foregoing considerations using basic transmission-line theory [4]–[6], we can write

$$V(-y) = V_{y1} \exp(j\beta y) + V_{y2} \exp(-j\beta y)$$
$$V(-x) = V_{x1} \exp(j\beta x) + V_{x2} \exp(-j\beta x) \quad (1)$$

$$\Gamma_x = |\Gamma_x| \exp(j\psi) = \frac{V_{x2}}{V_{x1}} \quad (2)$$

$$\Gamma_D = |\Gamma_D| \exp(j\varphi) = \frac{V_{y2}}{V_{y1}} \quad (3)$$

$$V_{x1} \exp(j\beta x) = V + V_{y2} \exp(-j\beta y) \quad (4)$$

$$V_{y1} \exp(j\beta y) = V + V_{x2} \exp(-j\beta x) \quad (5)$$

Manuscript received January 21, 1974; revised March 11, 1974.
The author is with the Centro de Investigaciones Fisicas, Serrano, 144, Madrid, 6, Spain.